WELDING RESEARCH

SUPPLEMENT TO THE WELDING JOURNAL, OCTOBER, 1981
Sponsored by the American Welding Society and the Welding Research Council

# The Use of TETIG Diagrams in High Temperature Brazing

*Tetig diagrams provide a basis for comparing brazing filler metals and for evaluating the efficiency of brazing filler metals in promoting eutectic-free joints*

BY R. JOHNSON

SUMMARY. A centerline of brittle phases can exist in a brazed joint to the detriment of the mechanical properties of that joint. By the use of a tube-in-tube specimen which incorporates a variable gap geometry, the gaps at which various nickel-based braze filler metals first form the centerline phases can be evaluated. By constructing "tetig" diagrams that depict the interrelationships between temperature, time, and gap, the optimization of brazed joints can be effected in a more quantitative manner than previously.

## Introduction

For fabrication purposes, welding is the most commonly adopted joining technique where a permanent joint is required. Brazing has been used essentially in joints that will be subjected to low stresses in service, and there are several advantages in brazing certain components. In high temperature operations the sealing of metallic and ceramic joints has been successfully accomplished (Ref. 1). Additionally, the joining of molybdenum and tungsten high temperature seals where a large difference in expansion coefficients exists has also been effected by brazing (Ref. 2).

The use of lower melting point filler metals for brazing can also mean that components with specifically controlled cast or wrought microstructures and grain sizes do not have their optimized mechanical properties destroyed, as would be the case in fusion welding. This is especially useful when carrying out in-service repairs, for example, as in the case of repairing nickel superalloy components in gas turbine engines (Ref. 3). Another application is seen in very thin section joints, where fusion welding would result in grain growth to the extent of exceeding the wall thickness; examples are seen in joining ferritic and stainless steel aero-engine components (Ref. 4) and in thermocouple attachment to nuclear reactor fuel elements (Ref. 5) for in-service temperature monitoring.

In almost all brazing applications, service stressing is not arduous even though the braze filler metal flow would produce smoothly blended surfaces at the outer ends of components being attached. This is in contrast to the extremely sharp weld toes that can result from fusion joining, in regions of very high residual stresses from the contraction forces generated on cooling. Brazed fillets may also be of use where highly corrosive environments exist and where stagnant trapped liquors can degrade to cause stress corrosion cracking and associated phenomena. The two exceptions to this trend, where brazing was used for cyclicly stressed components, have involved:

1. Austenitic/ferritic steel transition joints in turbines (Ref. 6).
2. LMFBR heat exchanger joints in the transformable 9 Cr-1 Mo ferritic steel (Ref. 7).

*Paper presented at the 12th International AWS-WRC Brazing Conference held in Cleveland, Ohio, during April 7-9, 1981.*

*R. JOHNSON is Senior Scientific Officer, Springfields Nuclear Power Development Laboratories, United Kingdom Atomic Energy Authority (Northern Division), Springfields, Salwick, Preston, United Kingdom.*

It can, of course, be argued that the service conditions in aero-engines and turbines are also arduous for the brazed joints in the rotors.

A possible reason for the reticence in using brazed joints under severe service stresses is that brazing filler metals tend to be either soft, solid substitutional single phase alloys, or they contain light element melting temperature depressants (in nickel this includes phosphorus, silicon and boron) that form very hard and brittle intermetallic phases. These phases often agglomerate along the centerline of the joints. Moreover, they can crack under high stresses, such as those inducing plastic flow in the surrounding soft filler metal, and thus lead to subsequent joint failure.

Although nickel silicides and borides were found along the centerlines of some LMFBR tubular brazed joints (Ref. 7), the fitness-for-purpose mechanical tests were all easily passed. Indeed, the steel tubing would distort or break before the brazed joint failed. This was because correct joint design had resulted in very low stresses being generated along the joint centerline, although high stresses were being applied to the joint as a whole. Under more arduous service conditions and in applications where the joint design is below the optimum (perhaps for reasons of accessibility), the centerline phases might become a liability.

A research investigation was begun to evaluate how the joint microstructure might be controlled and improved. It was apparent from the existing literature that little guidance was available, apart from the ubiquitous joint recommendation of about 50 μm (0.002 in.) with a brazing temperature range up to 120°C (248°F) with some filler metals and no guidance as to the necessary soaking time at temperature. This paper describes the work to date in establishing how the joint microstructure in some nickel-based filler metals can be controlled, and what further work is necessary for a quantitative analysis to be made.

## Previous Assessment Work

The braze filler metal chosen for the LMFBR 9 Cr-1 Mo tube-tube joint work was BNi4 (Ref. 7); the solidification sequences of this and the other candidate filler metal, BNi2, have been extensively studied by optical and electron microscopy (Ref. 8).

The initial phase formed in BNi4 on cooling is α-nickel in the form of dendrites growing from the joint sides. As these grow, the remaining molten filler metal becomes enriched in boron because only silicon is contained in solid solution in the α-nickel. At a critical concentration, nickel boride begins to form at the same time as the α-nickel (i.e., a eutectic valley in the phase diagram is reached). Since the boride contains no silicon, the latter element becomes more concentrated in the remaining liquid. When the final eutectic is reached, nickel silicide and nickel boride are formed as a finely integrated structure.

As can be seen in Fig. 1, up to three phases can exist in a BNi4 joint. BNi2 contains an additional eutectic between α-nickel and chromium carbide prior to the onset of nickel boride formation (Ref. 8).

By using different temperatures and soak times, it was established that the number of phases in the joint could be reduced. In the tubular joints, the effect of tilting the inner tube axis away from that of the outer tube also affected the joint microstructure; the controlling influence is seen to be the boron content of the joint as defined by the original gap. If the boron level is limited, the ternary eutectic will not be attained and no silicide will be formed. This is because the volume fraction of boride is not sufficient to raise the silicon content in the remaining molten filler metal above the solid solubility limit in α-nickel. As a result, only two phases exist in the joint—the α-nickel and the nickel boride. More extensive boron diffusion into the steel is rapid at brazing temperatures and will eventually denude the joint region of boron completely; a single phase of α-nickel will then grow to fill the joint.

The problem with centerline eutectics containing hard, brittle compounds can be seen in Fig. 2. There a wide eutectic shows a multiplicity of crack paths in Fig. 2A, although a very narrow but continuous centerline eutectic can still crack progressively as in Fig. 2B. In order to

*Fig. 1—Electron micrograph of BNi4 joint in 9 Cr-1 Mo steel. X800 (reduced 55% on reproduction)*

eliminate the centerline of brittle phases, a combination of three conditions must occur:

1. The temperature of the brazing operation must be high enough so that the boron contained within the joint diffuses into the substrate during the brazing cycle.
2. The time of the soaking at temperature must be sufficient to permit the requisite amount of boron diffusion to occur during the brazing cycle.
3. The gap within the joints must be such that the amount of boron contained therein can be eliminated during the brazing cycle.

From the first letters of these related variables—Temperature, Time, and Gap—the work TETIG was coined. A tetig diagram is thus one which, in two dimensions, has two of the variables along the axes of the graph, while variations in the third produce a family of curves.

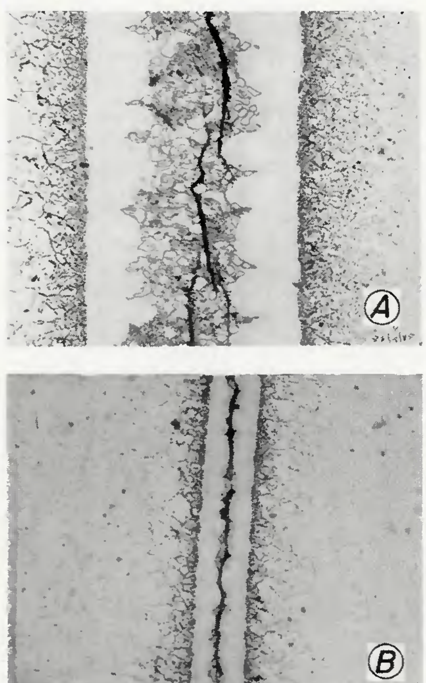


*Fig. 2—Centerline cracking in BNi4 joints. X200 (reduced 50% on reproduction)*

The initial assessment utilized the tilted tubular specimens in 9 Cr-1 Mo steel to extrapolate data to zero centerline eutectic (Ref. 9). A later paper extended this data to a comparison of flat plate and tubular specimens (Ref. 10). The difficulties in accurately maintaining the joint gaps in the flat plate specimens led to the reassessment of tubular specimens, with predetermined rather than unprogrammed and random offsets. Figure 3 is derived from a compilation of this previous work; it shows schematic and actual tetig diagrams with the gap and temperature plotted along the axes and thus has time as the third variable.

## Experimental

### Braze Filler Metals

BNi2 and BNi4 filler metals were obvious choices. In addition, BNi3 which contains no chromium and less iron, was chosen for comparison to BNi2. Additionally a silicon-free filler metal, NK10 (British Standards), was also assessed in order to ascertain whether or not a simple boron-containing filler metal gave better results.

The compositions of all form filler metals are given in Table 1, along with the solidus and liquidus temperatures. It can be seen that silicon-boron filler metals benefit from additions of chromium in causing the liquidus to fall to the minimum value seen in BNi2; also, the silicon-free filler metal has an appreciably higher solidus than the other three.

All filler metals were obtained from Wall Colmonoy, UK, as Nicrobraz powders LM, 130, 135 and 150. They were mixed with residue-free acrylic binders to form a paste which was placed in the bottom of the alumina crucibles used to contain the tubular specimens.

### Base Metal and Specimen Design

Although the initial work had been performed on 9 Cr-1 Mo tubing and flat sheet, the former was available in only a limited range of sizes. Accordingly, for this basic assessment it was decided to use AISI 321 austenitic stainless steel, which is readily available in a large range of tube sizes.

With the experience of the tilted 9 Cr-1 Mo tubes, it was possible to derive a specimen that had an axially offset tube within a tube, i.e., the tubes touched along their length rather than at two diametrically opposite points. The specimens in Fig. 4 are similar to those suggested for the capillary flow assessment of solders and brazes (Ref. 11). However, the Fig. 4 specimens have larger diameters and smaller maximum gaps in order to decrease the rate of change of joint gap with rotation around the circumference. The specimens were measured to be within the tolerances quoted in Fig. 4, and the inner tube

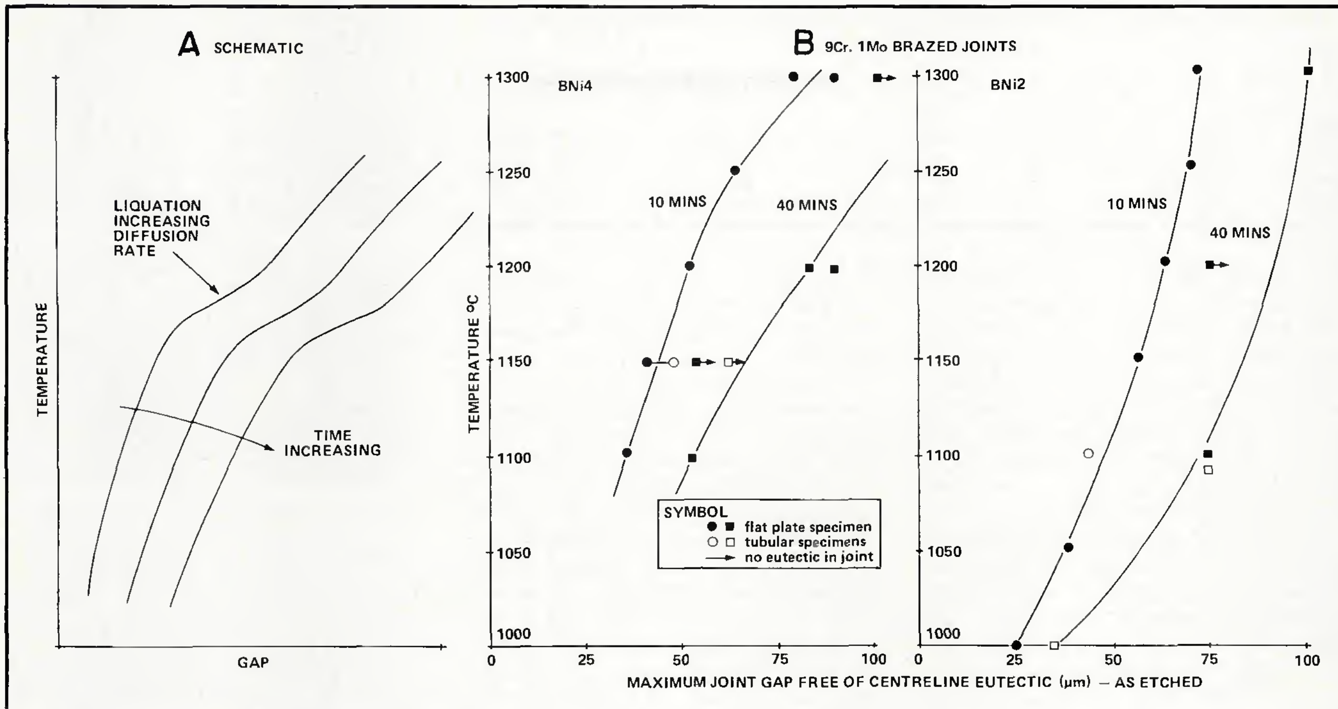


*Fig. 3 — Tetig diagrams derived from previous work*

locked tight against the outer tube by means of the two M4 grub screws. The joint gap produced varies from zero to the diametrical difference between the inner and outer tubes, and this can be calculated for any position around the circumference (see Appendix).

**Brazing Cycle and Examination Procedures**

The specimens were placed vertically in the crucibles containing the different filler metals. The crucibles were then inserted into a vertical position cold-walled vacuum furnace. After evacuation to $10^{-4}$ torr the temperature was raised at a rate of 1°C/second (s) (1.8°/s) to 900°C (1,652°F), whereupon a 5 minute (min) temperature equalization hold was effected. The furnace was raised to the brazing temperature also at a rate of 1°C/s (1.8°F/s), and the soak time started as soon as the thermocouple adjacent to the specimens attained a temperature within 5°C (9°F) of the present level (30-60 s) before the plateau was reached. The brazing temperature was maintained to within ±3°C (5°F). After completion of the soak time, the furnace heaters were switched off and the chamber allowed to cool naturally to 800°C (1,472°F). At this point, an argon gas assist was initiated to bring the furnace quickly back to room temperature.

After an initial run for 10 min the top

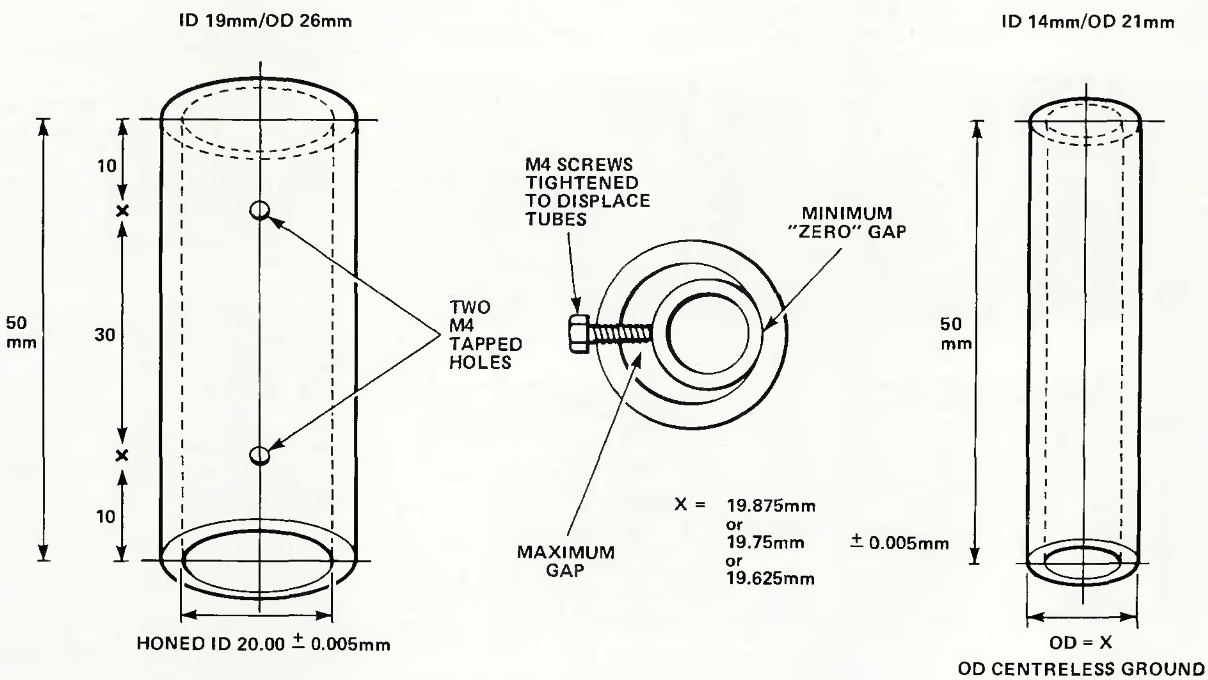


*Fig. 4 — Tubular brazing specimens made from AISI 321 stainless steel stock*

Table 1—Compositions of Braze Filler Metals, (wt-%) with Solidus and Liquidus Temperatures

| | Ni | B | Si | Cr | Fe | Solidus °C (°F) | Liquidus, °C (°F) |
|---|---|---|---|---|---|---|---|
| BNi2 | Bal | 3.1 | 4.5 | 7.0 | 3.0 | 970 (1778) | 1000 (1832) |
| BNi3 | Bal | 3.1 | 4.5 | — | 0.5 | 980 (1796) | 1040 (1904) |
| BNi4 | Bal | 1.9 | 3.4 | — | 1.5 | 990 (1814) | 1060 (1940) |
| NK10 | Bal | 3.6 | — | 15.0 | 1.5 | 1055 (1931) | 1055 (1931) |

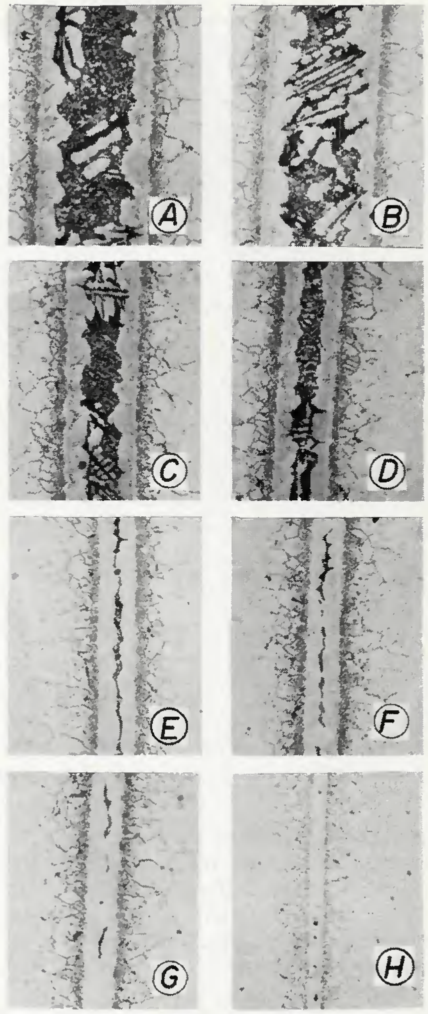

*Fig. 6 — Variations in microstructure with gap around circumference of a NK10 joint. ×200 (reduced 50% on reproduction)*

6-7 mm (0.24-0.28 in.) of each specimen was removed by a disc slitting wheel for metallurgical preparation and examination. The specimen was returned to the furnace for the next additional soak time, although, with each subsequent brazing run, no new brazing filler metal was added. The sectioning procedure was repeated and the specimen returned to the furnace for further soaking.

Each section was mounted in Bakelite and polished to 1 $\mu$m diamond finish prior to etching electrolytically at 4.5 V in 10% oxalic or 5% sulphuric acid etches. The optical metallography was conducted on a Reichert MeF projection microscopic, mainly at ×200, with a special attachment that permitted the specimen to be revolved over the objective lens. The final (etched) joint gaps were measured to ±0.5 $\mu$m where the centerline eutectic started and where it became continuous; the angular displacements around the joint circumference between these positions were measured to ±1 deg at each position.

## Results

Examples of four braze filler metals can be seen in Fig. 5. It can be seen that BNi4 has the three phases described previously; in addition to the three phases, the other filler metals also have a fourth phase in the black-and-white $\alpha$-nickel/chromium carbide eutectic regions. NK10 also shows no sign of separate nickel boride particles, the intermetallic being presumably contained within the fine microstructure along the central region of the joint.

Figure 6 depicts the manner in which the joint microstructure varies around the circumference from close to the maximum gap to adjacent to the minimum. From a large gap where the $\alpha$-nickel/chromium carbide eutectic bridges the centerline eutectic only occasionally, the gap narrows down to where it divides regions of eutectic by a considerable distance. It should be remembered that this is a planar section through the joint, and that above and below this plane the regions of eutectic will, in all probability, still be continuously linked (e.g., Figs. 6C and D). Eventually the centerline eutectic becomes so thin that breaks become apparent (Fig. 6F) and the line disappears altogether (Fig. 6G). Thereafter any particles within the joint other than the $\alpha$-nickel cannot be regarded as part of a widely-disjointed centerline eutectic. It is also notable that the individual fields of view of more than about 0.4 mm (0.016 in.) show little indication of a tapering joint gap — something that the tubular specimens were designed to achieve.

The effects of hold time are depicted in Fig. 7. Here the BNi2 joints show both a marked increase in the $\alpha$-nickel width adjacent to the steel and a large increase in the boron diffusion into the steel where iron and chromium borides will be formed along the grain boundaries (Ref. 8).

The effect of brazing temperature can be seen in the pictures of BNi4 joints (Fig. 8). The appearance of the first three pictures (Figs. 8A, B, C) is comparable with the hold time effect — the $\alpha$-nickel region increases in depth with rising temperature, as does the extent of diffusion. But at 1250°C (2282°F) the microstructure changes markedly, and the magnification of Fig. 8D at ×100 is only half of that of the other three.

As shown in Fig 8D, at 1250°C (2282°F) the grain boundaries have liquated so that the grain boundary penetration has increased greatly. In addition, the central zone of the joint has become full of a different type of eutectic or indeed isothermal compound formed by the interdiffusion of the braze filler metal and steel elements. Previously with 9 Cr-1 Mo joints, the liquation "joint line" was discernible because of a non-etching phase being formed in the martensitic steel; with AISI 321 no such boundary is

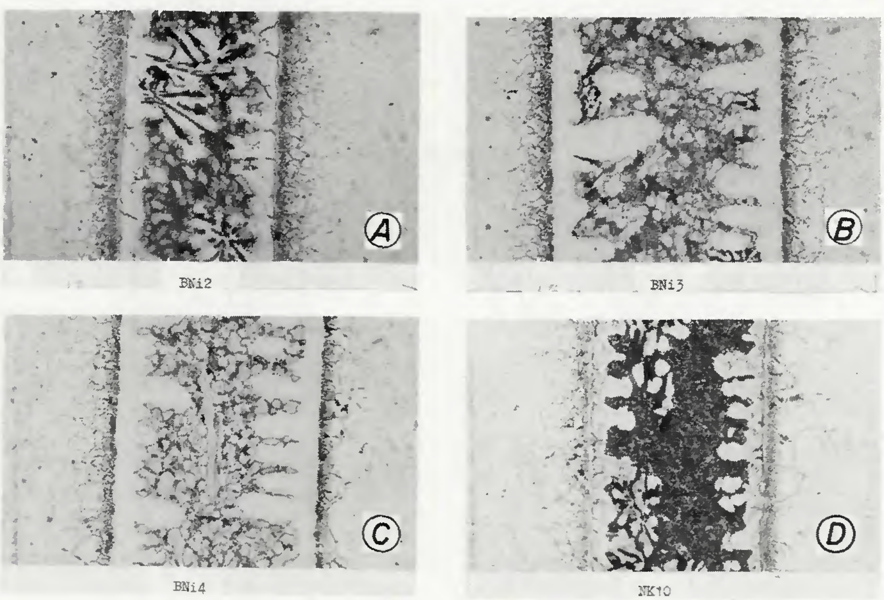

*Fig. 5 — Typical joint microstructures: A — BNi2; B — BNi3; C — BNi4; D — NK10. ×200 (reduced 50% on reproduction)*

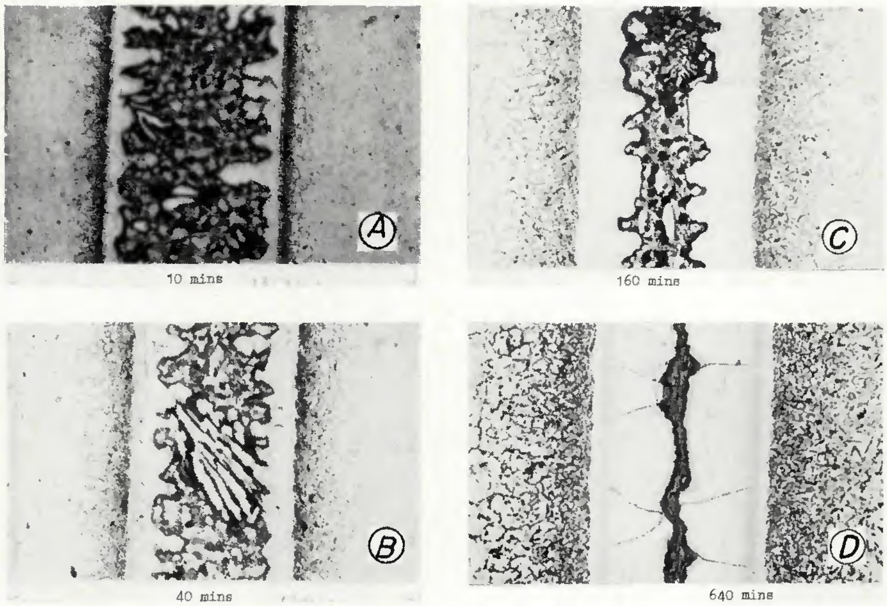


*Fig. 7 — Effect of hold time on joint microstructure: A — 10 min; B — 40 min; C — 160 min; D — 640 min. X200 (reduced 50% on reproduction)*

visible. Thus, there are no joint data comparable to those at lower temperatures with regard to etched final gaps, although at a certain point around the circumference the center phase became discontinuous and disappeared in a manner similar to the lower temperature specimens. Thus, the angular measurements could still be made. However, with the dramatic change in microstructure, it is unlikely that the values produced will bear much relation to the other data.

## Discussion

### Presentation of Results

Although the results had been presented previously as tetig diagrams with time as the third variable, the initial high temperature results indicated that for two brazing filler metals (BNi4 and NK10) there was to be a more limited temperature range in which data could be collected — namely, 1100-1200°C (2012-2192°F). Even BNi2 and BNi3 could only be used at temperatures slightly below this range because of their lower melting points, whereas the time varied from 10 to 640 min. Indeed, the times had been chosen with 10 min as a minimum realistic vacuum furnace heat treatment time, and each subsequent time was a factor four higher than the previous one.

Depth of penetration of a substitutionally diffusing species, $\chi$, is related to the diffusion coefficient, D, and time, t, by $\chi = \text{const.} \sqrt{D.t}$ (Ref. 12). This, in turn, implies that the times selected will roughly double up the penetration of the braze filler metal elements into the steel. The amount of remaining centerline eutectic will obviously be related to the amount that has diffused into the steel.

Boron segregates strongly to the grain boundaries where diffusion is known to be more rapid than through the bulk grains. As a result, it would be interesting to determine the power relationship between the joint gap and the time. Indeed, a log · log plot would also foreshorten the range in times to be plotted. As the temperatures have been selected at discrete levels and the joint gaps vary indefinitely, it is also useful that the third variable has a restricted number of levels. Unless this occurs, the family of curves becomes intermingled because of experimental scatter. Thus, the tetig diagrams are drawn as log · log plots of gap against time with temperature as the third independent variable.

### Final Joint Gap TETIG Diagrams

Figure 9 summarizes the tetig diagrams for the first centerline eutectic, and Fig. 10 those for the first continuous centerline eutectic — both sets of results being taken from joint gaps measured after brazing. It is notable that only data below 1250°C (2282°F) are included; this is because joint gaps were not discernible in the highest temperature specimens.

Figures 9 and 10 show the higher temperatures consistently produce wider eutectic-free joint gaps, and that the gradients of the log · log plots are close to and slightly less than 0.33. It has been suggested (Ref. 13) that grain boundary diffusion can be related by a 0.33 power law, and the small increase seen in the gradients of the plots above 0.33 may be attributed to the additional effects of the silicon and nickel substitutional diffusion on top of the basically grain boundary diffusing boron. Indeed, at high temperatures boron itself is thought to diffuse through bulk grains as well as along the grain boundaries (Ref. 14). The fact that the $\alpha$-nickel layer is increasing by isothermal solidification during the hold time may also serve to slow down the boron diffusion; this is because it may act as an additional barrier with diffusion confined to the interdendritic boundaries.

Although two joint gaps have been used in the specimens from which these plots have been derived, there appears to be little effect on the results. At 1150°C (2102°F) the 125 and 250 $\mu$m joint gap specimens are in very good agreement. Also, with the very slowly tapering joint gap, any doubts as to the position of the first centerline eutectic or the first continuous centerline eutectic do not affect the measured gap greatly — by little more than 1 $\mu$m in most cases. With the machining undulations and the discrete way in which solidification in small gaps occurs, the accuracy is very good.

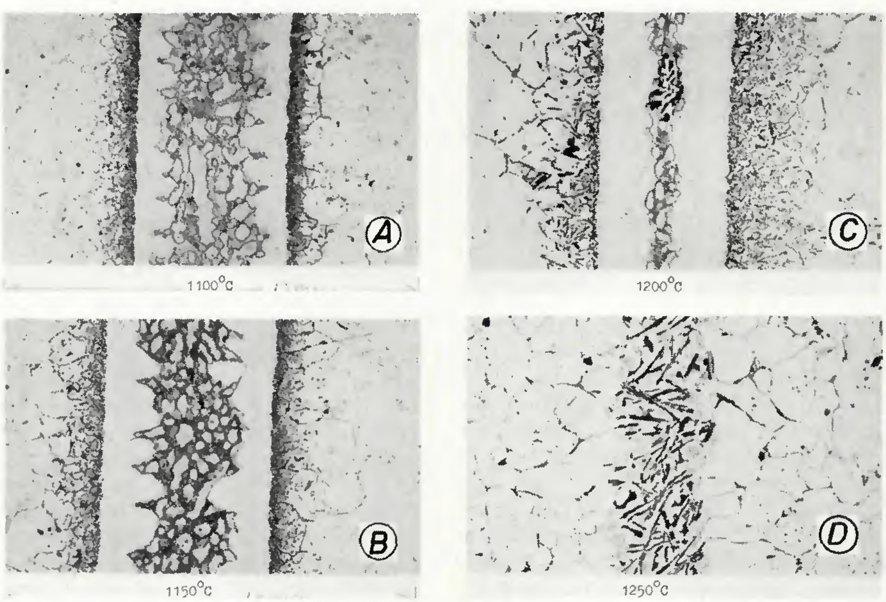


*Fig. 8 — Effect of brazing temperature on joint microstructure: A — 1100°C (2012°F); B — 1150°C (2102°F); C — 1200°C (2192°F); D — 1250°C (2282°F). Magnifications as follows: A, B, C — X200; D — X100 (all reduced 50% on reproduction)*

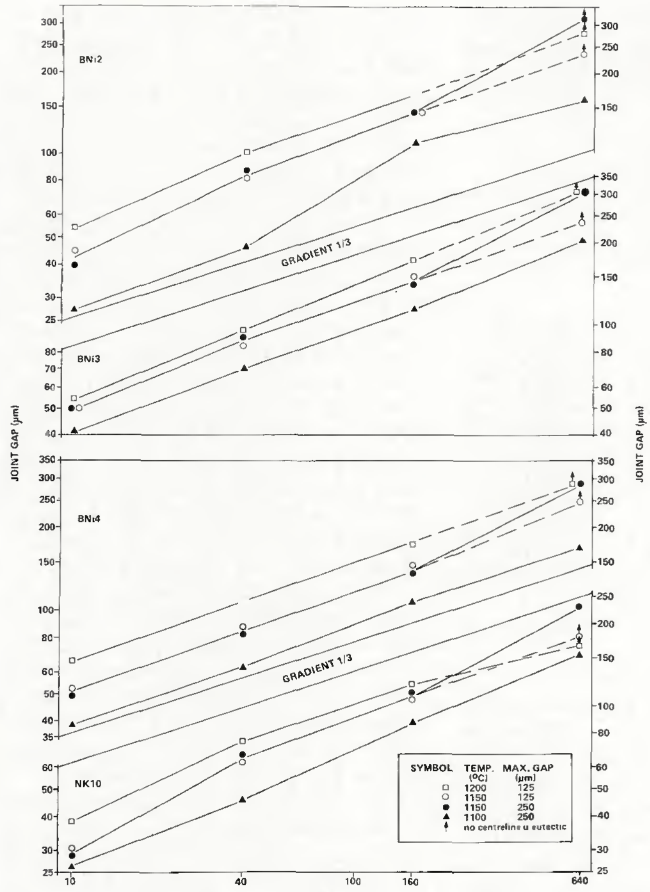

*Fig. 9—Final etched joint gaps—first centerline eutectic*

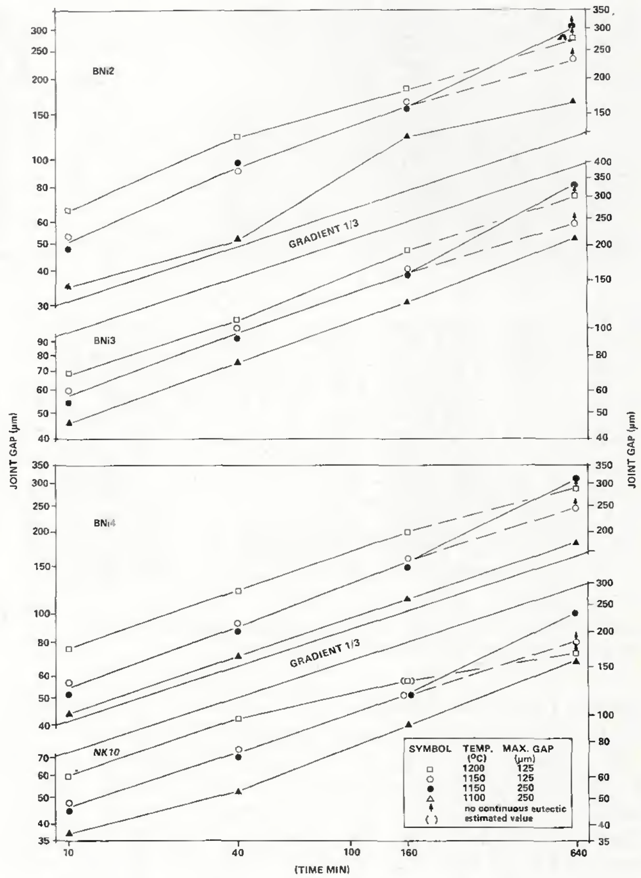

*Fig. 10—Final etched joint gaps—first continuous centerline eutectic*

**Original Joint Gap TETIG Diagrams**

Figures 11 and 12 show the tetig lines for the original joint gaps. These are derived from the angle subtended at the center of the specimen by the two extremities of the continuous centerline eutectic, as can be seen in Fig. 13.

There are several differences between Figs. 11 and 12 and Figs. 9 and 10 as well as certain similarities. The general gradient is still about 0.33. Also, there is a reasonably consistent increase in angle subtended by the arms of the centerline eutectic—and hence the prior gap present—as the time increases at constant temperature. The differences are that the data from the selected temperatures overlap in terms of original gaps in contrast to the clearly segregated data on the etched gaps, and that inherently more scatter is discernible.

This is not too surprising when the method of measurement is analyzed. An error of $\pm 1$ deg for each arm of the centerline eutectic accumulated to $\pm 2$ deg in total, and for a 250 $\mu$m gap specimen this correlates with gaps measured to $\pm 4.4$ $\mu$m. Also, the specimens were designed such that any areas of doubt as to the exact location of the ends of the centerline eutectic arms, with small local perturbations in joint gap from machining or slight alloy composition differences, would be minimized in terms of measured joint gap because the rate of change of measured gap was so slow. In terms of rotation, however, these doubts will add to the errors of measurement. Thus together, these factors will result in more scatter in this diagram than is seen in the diagram for etched gaps. In this context the field of view, approximately 0.4 mm, is equivalent to 2 deg rotation of the specimen.

Further work is planned to assess more definitively the original joint gap data by means of larger diametrical differences. The diametrical difference can be increased to the point where a lack of braze flow occurs due to the reduction in capillary forces in the joint. If this is done, then the outer tube diameter can be decreased so that the same diametrical difference in a smaller specimen will lead to more rapid changes in gap with angular rotation. It is interesting to note that the capillary specimen design used diameters of 14 and 13.5 mm (Ref. 11).

A further complication is some evidence that the dissolution of the substrate by the braze filler metal is dependent on the original gap. It can be seen in Fig. 12 that the 250 $\mu$m specimen data at 1100°C (2012°F) lie very close to the 125 $\mu$m specimen data at 1150°C (2102°F), and similarly with the 250 $\mu$m/1150°C (2102°F) and 125 $\mu$m/1200°C (2192°F) data. If this effect is found to be pronounced, then the variable gap specimen concept requires additional quantification, unless the rate of change in gap with angle is very low.

This effect will be investigated by using wider gaps than cited in this paper in an attempt to quantify its magnitude. In the etched gaps there was less tendency towards any enhanced dissolution at wider gaps (comparing the sets of data for 1150°C i.e., 2102°F), and not to the extent that this caused extensive overlap of data at different temperatures. In this context specimens must be measured before brazing because the machining tolerances can also add to the errors discussed hitherto.

In Figs. 11 and 12 the data from the 1250°C (2282°F) specimens are recorded, where no equivalent data can be plotted for the etched gaps. The increase in temperature has not resulted in an increase in equivalent gap, but rather the reverse is true. However, it must be remembered that the 1250°C (2282°F) specimens showed a marked change in joint morphology (Fig. 8) with a dark etching phase exclusively occupying the joint centerline. With the onset of grain boundary liquation; in iron and 9 Cr-1 Mo steel at about 1175°C (2147°F), and in

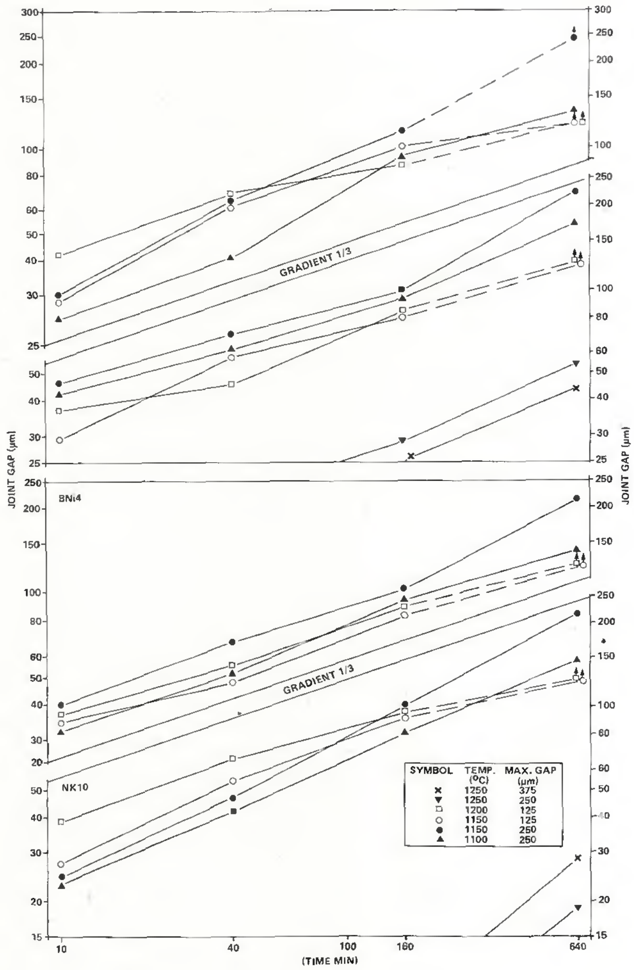


*Fig. 11 — Original joint gaps — first centerline eutectic*

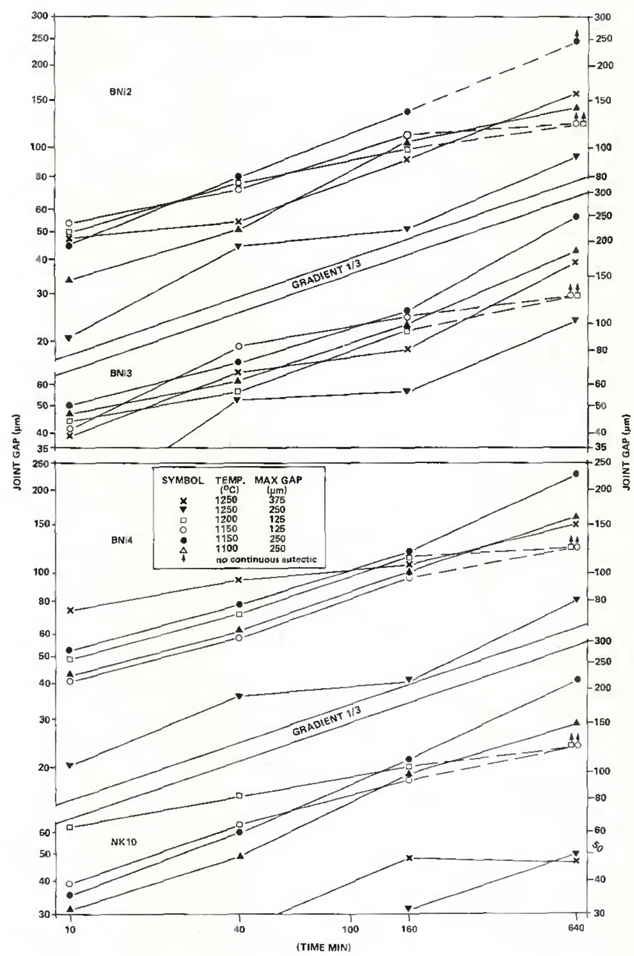


*Fig. 12 — Original joint gaps — first continuous centerline eutectic*

AISI 321, the microstructures in the 1200°C (2192°F) specimens show that this temperature is close to the liquation point; interdiffusion of braze filler metal and substrate elements are greatly increased. This means that chromium (and titanium) will be able to diffuse into the joint region more rapidly than below the liquation temperature; also, any carbon tied up as carbides in the grain boundaries will similarly enter the joint.

The phase is probably a chromium boro-carbide (Ref. 8). It is much more stable than iron boride, the eutectic temperature in the chromium-boron binary phase diagram being at about 1620°C (2948°F) rather than 1175°C (2147°F) for iron-boron. Thus, the longer centerline eutectic arms may be caused by the increase in chromium (and titanium) diffusion rates; these tie up the boron and any carbon *in situ* rather than allowing the diffusion of the boron into the steel that is seen at lower temperatures.

The calculation of the original gap is expounded in the Appendix. It is based on a cosine relationship rather than a simple angular relationship. The measurements are made by keeping the joint centrally disposed in the viewing screen, i.e., effectively following the path of the intermediate circle.

**Differences Between Braze Filler Metals**

The filler metals fall into three categories:

1. High silicon/boron (4.5/3.1 as in BNi2 and 3).
2. Lower silicon/boron (3.4/1.9 as in BNi4).
3. High boron alone (0/3.6 as in NK10).

If the boron diffusion governs the joint microstructure, then the filler metal with the lowest level of boron should be first to become eutectic-free along the joints. In the etched joints gap data, BNi4 fulfills this prediction.

BNi2 and 3 are very similar but slightly less efficient in losing boron than BNi4. NK10 is appreciably less efficient in removing the boron from the joint and the centerline into the steel. Thus, it might be concluded that the presence of silicon is synergistic to boron diffusion. However, the addition of 15% chromium to NK10 is far higher than that seen in the other filler metals, and this may also affect the diffusion characteristics.

The effect is certainly not caused by different dissolution rates of the substrates by the filler metals, because the original joint gap data mirror the effect discussed above for etched joints. Interestingly, the 1250°C (2282°F) data for NK10 are far below the lower temperature data and below the data from the other filler metals. Also, the 15% chromium pre-existing within the filler metal may add to the tying up of the boron within the joint, whereas the other filler metals rely more exclusively on the chromium and other steel elements diffusing into the joint.

**Uses of the TETIG Diagrams**

It has been suggested earlier in this paper that the eradication of centerline eutectics would result in tougher brazed joints, with crack propagation hindered by the crack having to pass through a ductile rather than a brittle phase. Certainly, the cracks introduced by the slitting method did not propagate beyond the regions of centerline eutectic (Fig. 2B), and earlier work on 9 Cr-1 Mo showed that the $\alpha$-nickel dendrites could act as effective crack arresters, and that cracks had to deviate around them (Ref. 8).

Some papers relating to the mechanical properties of brazed joints have not consistently found this. Weiss *et al* (Ref. 15) attempted a prolonged high temperature treatment of a BNi5 joint. However, as the joint etched up to 170-190 μm the centerline eutectic phases were not eliminated by the soak at 1100°C (2012°F). Lugscheider (Ref. 16) has noted that the presence of centerline phases is not solely dependent on temperature and time—that is, when using flat plate standard joint gap (25 $\mu$m) specimens.

It is known that flat plates can distort during a furnace heat treatment, so that some variation in joint gaps can result. From Lugscheider's data (Ref. 16), however, the hard phases did decrease consistently with increasing temperature when only 0.5% P is present. Moreover, the filler metals containing 3% P show an intermediate maximum in the graphs of percentile phases vs. temperature. However, the system is more complex than the Ni-Si-B system, where the major temperature depressant is boron which forms only intermetallics, and where the secondary depressant is silicon which can be contained in $\alpha$-nickel solid solution. The boron is the faster-diffusing species, but in the other system the major depressant and compound-former (phosphorus) is slower at diffusing than silicon. Therefore, the changes in joint metallurgy as diffusion increases with temperature may be more complex than those in the Ni-Si-B systems.

As suggested in his paper, each filler metal/base metal pair selected must be investigated separately. However, Lugscheider confirmed that the better tensile properties were always associated with the least amount of centerline phases. Even earlier work on the effect of time and temperature at Springfields showed that the tensile strengths and remelt temperatures of brazed joints increased with temperature (Ref. 17).

It is seen that the elimination of the centerline eutectic can result in improved mechanical properties. If this is predictable, then suitable brazing/heat treatment cycles can be adopted to do it. It is probable that the first eutectic visible is a more critical criterion for crack arresting, because it must be remembered that the analysis is based on a planar section through the joint. Apparently, divided regions of eutectic may in fact be linked by eutectic regions above and below this plane.

In terms of total joint failure the breakup of a continuous centerline eutectic means that the whole joint will not crack easily and that the gaps between eutectic islands will act as crack retarders. Thus, it is unlikely that even a leak path will be generated when the joint is not cracking along its whole length (i.e., the crack opening displacement will be reduced). Despite this, the first eutectic would always serve as a more conservative estimate.

In terms of etched gaps, a 100 $\mu$m gap is rendered eutectic-free by brazing as follows:

1. BNi4—1200°C (2192°F) for 30 min or 1150°C (2102°F) for 65 min or 1100°C (2012°F) for 135 min.

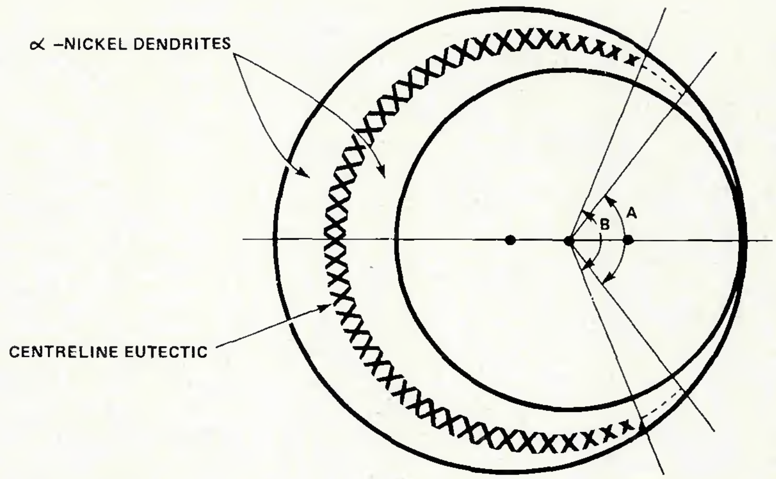


Fig. 13—*Angles subtended by the centerline eutectic: A—angle subtended by first eutectic; B—angle subtended by first continuous eutectic. Angle subtended at center of the intermediate circle, radius ½($R_1$ + $R_2$) and center midway between centers of tube circles; gaps are calculated at A/2 and B/2, assuming that the centerline eutectic is distributed symmetrically about the contact point of the two tubes.*

2. BNi2—1200°C (2192°F) for 40 min, 1150°C (2102°F) for 60 min, and 1000°C (2012°F) for 155 min.

The ubiquitous 50 $\mu$m gap is eutectic-free after 10 min at either 1200 or 1150°C (BNi2 and 4), and 1100°C for 17 min (BNi4) and 1100°C for 35 min (BNi2). If the dissolution effects were quantified, then the etched gaps would be converted into original gaps. However, even with data to date, the BNi2 original gap data place the requirements at 1200°C for 15 min, 1150°C for 25 min, and 1100°C for 55 min. The BNi4 data are less consistent due to the more apparent effect of overall joint gap on increasing the scatter therein.

The tetig diagrams can also provide a useful basis for the comparison of different brazing filler metals; the diagrams can also keep in an evaluation of the efficiency brazing filler metals in promoting a eutectic-free joint. There will undoubtedly be some scatter in the data collected on the various braze filler metals. However, if the data-base of these diagrams is expanded, then more confidence can be used in predicting the requirements of temperature, time and gap in order to produce an optimized brazed joint. In agreement with Lugscheider, changes in the base material are equally as important as changes in the braze filler metals. Each system should be investigated to ensure there are no unforeseen morphological changes, such as liquation, occurring.

## Conclusions

This paper has reviewed the work on assessing how the centerline eutectic can be eliminated within a brazed joint. By using a tube-tube specimen with variable gap geometry the critical gaps at which the centerline eutectic begins to break up—and also disappears completely—can be measured and calculated. By plotting the results on a tetig diagram the effects and interactions of temperature, time and gap can be evaluated and used to predict how to optimize further joints.

*Acknowledgments*

The author wishes to thank his colleagues at Springfields for their help in compilation of this paper, and also particularly Mr. J. Elliott (British Aerospace) and Dr. H. Hughes and Mr. I. Bretherton for their contributions on the joint gap calculations.

*References*

1. Canonico, D. A., and Slaughter, G. M. 1978. Direct brazing of ceramics, graphite and refractory metals. Paper B-2A presented at 10th International AWS-WRC Brazing Conference, April 4-6, 1978, New Orleans, Louisiana.

2. Lundberg, L. B.; Turner, W. C.; and Hoffman, C. G. 1978. Brazing molybdenum and tungsten for high temperature service. *Welding Journal* 57 (10): 311-s to 318-s.

3. Chasteen, J. W., and Metzger, G. M. 1979. Brazing of Hastelloy X with wide clearance butt joints. *Welding Journal* 58 (4): 54-s to 58-s.

4. Doyle, J. R.; Eng, R. D.; and Ryan, E. J. 1977. Nickel-base brazing filler metals for aircraft and gas turbine applications. *Welding Journal* 56 (10): 15-21.

5. Sheward, G. E. 1970. Brazing applied to the development and manufacture of nuclear fuel elements. *Welding Journal* 49 (7): 548-558.

6. Heap, H. R., and Riley, C. C. 1971. Development of brazed austenitic/ferritic steel steam pipe joints for turbines. *Welding Journal* 50 (6): 253-s to 260-s.

7. Taylor, A. F., and Hayden, O. 1979. High integrity steam generator tube/tube plate joints for the LMFBR. *Welding Journal* 58 (12):

30-37.
8. Johnson, R. 1978. Microstructural aspects of brazing a ferritic steel with two Ni-Si-B braze filler metals. *Welding Journal* 57 (4): 93-s to 102-s.
9. Johnson, R., et al. 1979. Brazed joint microstructures of some nickel-based filler metals. Paper 21 read at Third International Brazing and Soldering Conference (BABS), October 1979, London.
10. Johnson, R., et al. 1980. Tetig diagrams help optimise brazed joints. *Welding and Metal Fabrication* 48 (8): 553-558.
11. International Standards Organization. 1977. *Solderability and brazeability — definition and use of a specimen with a variable gap.* ISO/TC44/SC3, N139.
12. Boler, R. M. 1951. *Diffusion in and through solids:* 247. Cambridge University Press.
13. Fleming, R. P. H. 1979. High temperature brazing and infiltration on some nickel-base alloy composites. 1979. Paper 19 read at Third International Brazing and Soldering Conference, October 1979, London.
14. Feduska, W. 1961. The nature of the diffusion of brazing alloy elements. *Welding Journal* 40 (2): 81-s to 89-s.
15. Weiss, B. Z.; Steffans, H. D., Engelhart, A. H. and Wielage, B. 1979. Static and dynamic crack toughness of brazed joints of Inconel 718 nickel base alloy. *Welding Journal* 58 (10): 287-s to 295-s.
16. Lugscheider, E.; Klohn, K. and Burchard, W. 1980. Structure of low-phosphorus alloyed nickel-chromium-silicon brazed stainless steel joints. *Welding Journal* 59 (10): 283-s to 288-s.
17. Sheward, G. E., and Adam, R. W. 1972. An investigation of remelt temperature changes in some commercially available filler metals. Paper 11 read at the First International Brazing and Soldering Conference (BABS), November 1972, London.

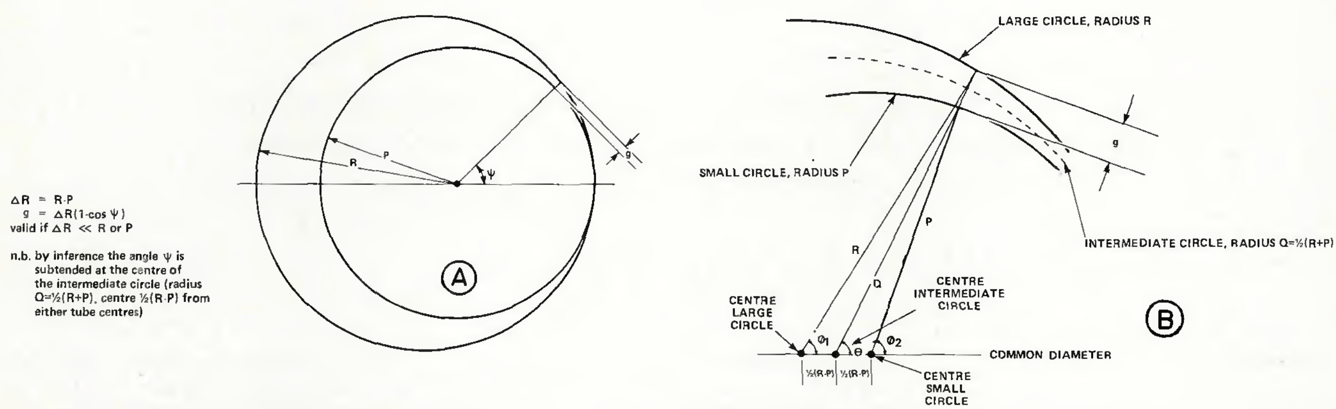


*Fig. 14 — Methods for calculating joint gap around variable gap specimen: A — Approximate method diagram; B — intermediate circle method diagram; C — outer circle closest approach method diagram*

## Appendix: Calculation of Joint Gap Around Variable Gap Specimen

The analyses are based on small circle, radius P, being contained inside a larger circle, radius R, and touching at one point. The simple approximation to calculate the joint gap (g) in terms of the difference in radii ($\Delta R = R - P$) is given by (see Fig. 14A):

$$g = \Delta R(1 - \cos \psi)$$

This is valid if $\Delta R \ll R$ or P, and effectively takes the angle $\psi$ at the half way point between the two circle centers. The equation has no rigorous proof, and based on the concept of an intermediate circle radius $Q = \frac{1}{2}(R + P)$ with its center midway between the two original circle centers a more complex set of equations is required (see Fig. 14B):

$$g = X - Y$$

where: $X^2 = Q^2 + 2R(R - Q)(1 - \cos\phi_1)$
$Y^2 = Q^2 - 2P(Q - P)(1 - \cos\phi_2)$

with: $\cos \phi_1 = (-B \pm \sqrt{B^2 - 4AC})/2A$
$\cos \phi_2 = (-E \pm \sqrt{E^2 - 4DF})/2D$

when: $A = R^2$
$B = -2R(R - Q)\sin^2\Theta$
$C = -(R^2 - \sin^2\Theta(Q^2 + 2R(R - Q)))$

and: $D = P^2$
$E = 2P(Q - P)\sin^2\Theta$
$F = -(P^2 - \sin^2\Theta(Q^2 - 2P(Q - P)))$

In the equations for $\cos \phi_2$ the sign $\pm$ must be + for $0 \leq \Theta \leq 90$ deg and − for $90 \leq \Theta \leq 180$ deg. This equation is valid if $R > 3P$.

With specimens to date, the approximate solution is perfectly adequate. The maximum difference between the two solutions is at $\psi,\Theta = 90$ deg, and at diameters 20/19.75 mm the error is 0.0025 $\mu$m with the change of gap per degree rotation being 2.2 $\mu$m. Even with diameters 20/18 the error is only 1.4 $\mu$m with the change of gap per degree at 17.5 $\mu$m. With the difficulty in angular measurement resulting in accuracies not much better than ±1 deg, it can be seen that the errors of angular measurement outweigh the errors in the gap calculation. As the smaller circle decreases in size, the errors increase — with the error being approximately equal to change of gap per degree at diameters 20/14.

In both analyses an intermediate circle is adopted (i.e., the joint gap is kept central in the field of view of the microscope), but this is valid because both tubes are of the same material. If tubes of different material were to be used, then (because the dissolution rates of each into the braze filler metal will be different) the etched joint will no longer be centrally displaced about the original joint gap. In this case either the inner or outer edge of the joint must be kept central in the field of view, as this will be parallel to the original position of tube surface. Then the angular rotation is taken about the center of the selected circle.

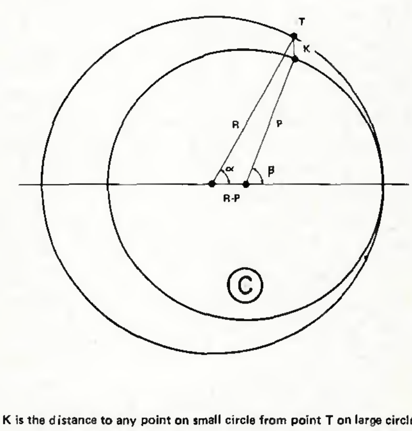


K is the distance to any point on small circle from point T on large circle.

Selecting the outer tube and rotating about its center an alternative approach is shown in Fig. 14C. A point is selected on the outer circle by defining the angle $\alpha$, and the distance K to the inner circle is calculated. By minimizing this distance, the closest approach (minimum joint gap) is evaluated:

$$K^2 = (P \sin \beta - R \sin \alpha)^2 + (P \cos \beta + R - P - R \cos \alpha)^2$$

With $\alpha$ selected the critical value of $\beta$ is given by

$$\tan \beta = (R \sin \alpha)/(R \cos \alpha - R + P)$$